BRAIN REPORT

Biallelic *NUDT2* variants defective in mRNA decapping cause a neurodevelopmental disease

Ralf A. Husain,[1,2,†] Xinfu Jiao,[3,†] J. Christopher Hennings,[4] Jan Giesecke,[5] Geeta Palsule,[3] Stefanie Beck-Wödl,[6] Dina Osmanović,[4] Kathrine Bjørgo,[7] Asif Mir,[8] Muhammad Ilyas,[8] Saad M. Abbasi,[8] Stephanie Efthymiou,[9] Natalia Dominik,[9] Reza Maroofian,[9] Henry Houlden,[9] Julia Rankin,[10] Alistair T. Pagnamenta,[11] Marwan Nashabat,[12] Waleed Altwaijri,[13] Majid Alfadhel,[12,14,15] Muhammad Umair,[12,14] Ebtissal Khouj,[16] William Reardon,[17] Ayman W. El-Hattab,[18,19] Mohammed Mekki,[19] Gunnar Houge,[20] Christian Beetz,[21] Peter Bauer,[21] Audrey Putoux,[22,23] Gaetan Lesca,[22,24] Damien Sanlaville,[22,24] Fowzan S. Alkuraya,[16] Robert W. Taylor,[25,26] Hans-Joachim Mentzel,[2,27] Christian A. Hübner,[2,4] Peter Huppke,[1,2] Ronald P. Hart,[3] Tobias B. Haack,[6] Megerditch Kiledjian[3] and Ignacio Rubio[5,28]

[†]These authors contributed equally to this work.

Dysfunctional RNA processing caused by genetic defects in RNA processing enzymes has a profound impact on the nervous system, resulting in neurodevelopmental conditions. We characterized a recessive neurological disorder in 18 children and young adults from 10 independent families typified by intellectual disability, motor developmental delay and gait disturbance.

In some patients peripheral neuropathy, corpus callosum abnormalities and progressive basal ganglia deposits were present. The disorder is associated with rare variants in *NUDT2*, a mRNA decapping and Ap4A hydrolysing enzyme, including novel missense and in-frame deletion variants. We show that these *NUDT2* variants lead to a marked loss of enzymatic activity, strongly implicating loss of NUDT2 function as the cause of the disorder. NUDT2-deficient patient fibroblasts exhibit a markedly altered transcriptome, accompanied by changes in mRNA half-life and stability. Amongst the most up-regulated mRNAs in NUDT2-deficient cells, we identified host response and interferon-responsive genes. Importantly, add-back experiments using an Ap4A hydrolase defective in mRNA decapping highlighted loss of NUDT2 decapping as the activity implicated in altered mRNA homeostasis.

Our results confirm that reduction or loss of NUDT2 hydrolase activity is associated with a neurological disease, highlighting the importance of a physiologically balanced mRNA processing machinery for neuronal development and homeostasis.

1 Department of Neuropediatrics, Jena University Hospital, 07747 Jena, Germany
2 Center for Rare Diseases, Jena University Hospital, 07747 Jena, Germany
3 Department of Cell Biology and Neuroscience, Rutgers University, Piscataway, NJ 08854, USA
4 Institute of Human Genetics, Jena University Hospital, 07747 Jena, Germany
5 Department of Anaesthesiology and Intensive Care Medicine, Jena University Hospital, Member of the Leibniz Center for Photonics in Infection Research (LPI), 07747 Jena, Germany

Received July 12, 2023. Revised November 08, 2023. Accepted December 05, 2023. Advance access publication December 23, 2023

6 Institute of Medical Genetics and Applied Genomics, University of Tübingen, 72076 Tübingen, Germany
7 Department of Medical Genetics, Oslo University Hospital, 0424 Oslo, Norway
8 Department of Biological Sciences, Faculty of Sciences, International Islamic University, Islamabad 44000, Pakistan
9 Department of Neuromuscular Disorders, UCL Queen Square Institute of Neurology, London, WC1N 3BG, UK
10 Department of Clinical Genetics, Royal Devon University Hospital, Exeter, EX1 2ED, UK
11 Oxford NIHR Biomedical Research Centre, Wellcome Centre for Human Genetics, Oxford, OX3 7BN, UK
12 Medical Genomics Research Department, King Abdullah International Medical Research Center, Ministry of National Guard Health Affairs, Riyadh 11426, Saudi Arabia
13 Department of Pediatrics, Neurology Division, King Abdullah Specialist Children's Hospital, King Abdulaziz Medical City, Ministry of National Guard Health Affairs, Riyadh 11426, Saudi Arabia
14 King Saud Bin Abdulaziz University for Health Sciences, Ministry of National Guard Health Affairs, Riyadh 11426, Saudi Arabia
15 Genetics and Precision Medicine Department, King Abdullah Specialized Children's Hospital, King Abdulaziz Medical City, Ministry of National Guard Health Affairs, Riyadh 11426, Saudi Arabia
16 Department of Translational Genomics, Centre for Genomic Medicine, King Faisal Specialist Hospital and Research Centre, Riyadh 11211, Saudi Arabia
17 Blackrock Clinic, Dublin, A94 E4X7, Ireland
18 Department of Clinical Sciences, College of Medicine, University of Sharjah, 27272, Sharjah, United Arab Emirates
19 Department of Pediatrics, University Hospital Sharjah, 72772, Sharjah, United Arab Emirates
20 Department of Medical Genetics, Haukeland University Hospital, 5021 Bergen, Norway
21 Centogene GmbH, 18055 Rostock, Germany
22 Groupement Hospitalier Est, Hospices Civils de Lyon, Service de Génétique, Centre de Référence Anomalies du Développement, 69677 Bron Cedex, France
23 Équipe GENDEV, Centre de Recherche en Neurosciences de Lyon, Univ Lyon, Univ Lyon 1, INSERM U1028 CNRS UMR5292, 69008 Lyon, France
24 Physiopathologie et Génétique du Neurone et du Muscle, Univ Lyon, Univ Lyon 1, CNRS, INSERM, UMR5261, U1315, Institut NeuroMyoGène, 69008 Lyon, France
25 Wellcome Centre for Mitochondrial Research, Translational and Clinical Research Institute, Faculty of Medical Sciences, Newcastle University, Newcastle upon Tyne, NE2 4HH, UK
26 NHS Highly Specialised Service for Rare Mitochondrial Disorders, Newcastle upon Tyne Hospitals NHS Foundation Trust, Newcastle upon Tyne, NE1 4LP, UK
27 Section of Pediatric Radiology, Department of Radiology, Jena University Hospital, 07747 Jena, Germany
28 Center for Sepsis Control and Care, Jena University Hospital, 07747 Jena, Germany

Correspondence to: Ignacio Rubio
Department of Anaesthesiology and Intensive Care Medicine
Jena University Hospital, Am Klinikum 1, 07747 Jena, Germany
E-mail: Ignacio.Rubio@med.uni-jena.de

Correspondence may also be addressed to: Megerditch Kiledjian
Department of Cell Biology and Neuroscience
Rutgers University, Piscataway, NJ 08854, USA
E-mail: kiledjian@dls.rutgers.edu

Keywords: Nudix; mRNA cap; Ap4A hydrolase; interferon; muscular hypotonia; basal ganglia

Introduction

Alterations in mRNA metabolism or mRNA translation are commonly associated with neurological disorders.[1] Accordingly, aberrancies in mRNA modifications can impact the stability and translation efficiency of mRNAs.[2,3] A key modification is the attachment of 5' cap structures to nascent mRNAs.[4,5] Capping protects mRNAs from degradation, increasing their lifetime, and also allows recognition by cap-binding proteins of the translational machinery.[6] Removal of the cap is catalysed by decapping enzymes, predominantly members of the Nudix (nucleoside diphosphate-linked moiety X) hydrolase superfamily[7,8] that exposes 5' mRNA termini to degradation by the exoribonuclease XRN1.[9] In addition to Nudix hydrolases, the Histidine-triad class of hydrolases primarily function on dinucleotides and include the DcpS scavenger decapping enzymes that cleave the residual cap structure following mRNA degradation from its 3' end.[10] A causal link between *DCPS* as well as the mRNA decapping enhancer EDC3 to neurodevelopmental disorders has been reported.[11-13] However, a link between members of the Nudix superfamily and human neuropathologies has not yet been rigorously established.

Perhaps the most compelling evidence for the involvement of Nudix-type hydrolases in neurodevelopmental disorders relates to *NUDT2* (Nudix hydrolase 2, MIM *602852), for which homozygous truncating variants have been reported in 10 individuals from six independent families with global developmental delay and

neuropathy (MIM #619844).[14-16] Based on these findings, a *NUDT2*-associated recessive neurological disorder has been postulated, but a link to changes in NUDT2 enzymatic activity was not reported.

The *NUDT2* gene is conserved across vertebrates but its specific function in human physiology remains unknown. Initially described as a hydrolase of the putative second messenger diadenosine tetraphosphate (Ap4A), NUDT2 was subsequently shown to also exhibit activity towards a broad range of capped substrates including m^7G-cap, unmethylated Gppp-, dpCoA- and FAD-capped RNAs.[17]

Here, we report novel rare damaging homozygous *NUDT2* variants and provide evidence from genetic, bioinformatic, cell-based and biochemical experiments that biallelic loss-of-function variants in *NUDT2* are causally linked to a neurodevelopmental syndrome.

Materials and methods

Additional methods are described in the online Supplementary material.

Patient enrolment and ethics

The cohort was assembled by consultations between collaborators (Families F1–F5, F7 and F9), using GeneMatcher[18] (Families F6 and F10) and ClinVar[19] (Family F8). Families F1 and F2 were previously reported,[14,15] but are included here because of fibroblast availability (Patient F1:II.5), to include an unreported sibling (Patient F2:II.3) and phenotyping of affected family members. The study was approved by the respective local institution's ethics committees and informed consent was obtained from all subjects or their guardians according to the Declaration of Helsinki.

Genetic testing

Exome genome sequencing and analysis were performed at Center for Genomic Medicine, Saudi Arabia; Tübingen University, Germany; Centogene, Germany; Genomics England, UK; Oslo, Norway; Bergen, Norway; Lyon University Hospital, France; and Queen Square Genomics, UK on genomic DNA from affected individuals.

Immortalization of patient fibroblasts

Human patient fibroblasts were cultured in Dulbecco's modified Eagle medium (DMEM) medium with D-glucose and pyruvate (Gibco) supplemented with 10% fetal calf serum (FBS, Gibco) and Penicillin/Streptomycin (Gibco). Fibroblasts were immortalized by transfection of SV40 large T antigen with FuGENE (Promega) according to the manufacturer's instructions and then split at a ratio of 1:2 for at least 10 passages before being considered immortalized. Control human fibroblasts were obtained from unaffected individuals for western blot analysis or Cellsystem Biotech for RNAseq analysis.

RNA generation and *in vitro* decapping assays

5' end triphosphate pcDNA3 polylinker RNA (pppG-pcP RNA) was *in vitro* transcribed from pcDNA3 polylinker PCR DNA template with T7 RNA polymerase (Promega, #P2075), as previously described.[20] ^{32}P-5' end labelled N7-methylated capped RNA was generated using the vaccinia virus capping enzyme[21] in the presence of [α-^{32}P]GTP and *S*-adenosyl-dismethionine (SAM), as described.[20] *In vitro* decapping assays were carried out by incubating 5' ^{32}P-cap labelled RNA with 50 nM recombinant NUDT2 wild-type or mutant proteins in 20 µl reaction mix containing 100 mM KCl, 2 mM $MgCl_2$, 4 mM $MnCl_2$, 2 mM DTT, 10 mM Tris-HCl (pH 7.5) at 37°C for 30 min. The decapping products were resolved by PEI-cellulose thin layer chromatography (TLC) plates (Sigma-Aldrich, #Z122882) developed in 0.45 M $(NH_4)_2SO_4$ at room temperature and visualized with Amersham Typhoon PhosphorImager.

Ap4A hydrolysis assay

Diadenosine tetraphosphate (Ap4A, 5 mM) (Sigma-Aldrich, #D1262) was incubated with 100 nM recombinant NUDT2 wild-type or mutant proteins in 20 µl reaction containing 100 mM KCl, 2 mM $MgCl_2$, 4 mM $MnCl_2$, 2 mM DTT, 10 mM Tris-HCl (pH 7.5) at 37°C for 60 min. Hydrolysed products were resolved by PEI-cellulose TLC plates (Sigma-Aldrich, #Z122882), developed in 0.45 M $(NH_4)_2SO_4$ at room temperature and visualized under short wave UV light.

Endogenous mRNA stability assay and qRT-PCR

Fibroblasts were cultured with DMEM/10% FBS medium. At 70% cell density, 5 µg/ml final concentration of Actinomycin D (Sigma-Aldrich, #A4262) was added to the medium to block RNA transcription. Total RNA was isolated with TRIzol™ reagent and treated with RNase-free DNase. Reverse transcription was performed on 2 µg of RNA with M-MLV reverse transcriptase (Promega, #M1701) and oligo(dT), according to the manufacturer's instructions. qRT-PCR was performed with the primers listed in Supplementary Table 1 and carried out on Applied Biosystems QuantStudio 3 Real-Time PCR (ThermoFisher) with iTaq SYBR Green Supermix (Bio-Rad Laboratories, #1725124). Relative mRNA levels were normalized to endogenous GAPDH mRNA.

Statistics

Gene expression differences were determined using pairwise Wald tests in DESeq2, corrected for multiple measurements with the Benjamini-Hochberg false discovery rate (FDR) (as adjusted *P*-value).

Results

Clinical characterization of individuals with homozygous *NUDT2* variants

We present findings from 18 individuals with homozygous *NUDT2* variants, from 10 different families [13 individuals from nine independent families previously unreported (Families F2–F10)], aged 3 to 21 years at last assessment. Common to all were symptom onset within the first 18 months of life, muscular hypotonia, motor developmental delay, gait disturbance and mild intellectual disability, with additional features like sensorimotor neuropathy present in some of the patients (Fig. 1A). Major clinical findings are summarized in Supplementary Table 2. Detailed clinical descriptions are provided as case reports in the Supplementary material. Cerebral MRI was available for review in 13 patients aged 5 months to 20 years at investigation. Partial agenesis and hypoplasia of the corpus callosum were present in nine individuals (Fig. 1B–D), delayed myelination in two individuals, and brain malformation in one individual (Fig. 1E). In four siblings (Families F2 and F3), bilateral-symmetric basal ganglia signal abnormalities were present, with findings being more pronounced in the older siblings (Fig. 1F–M).

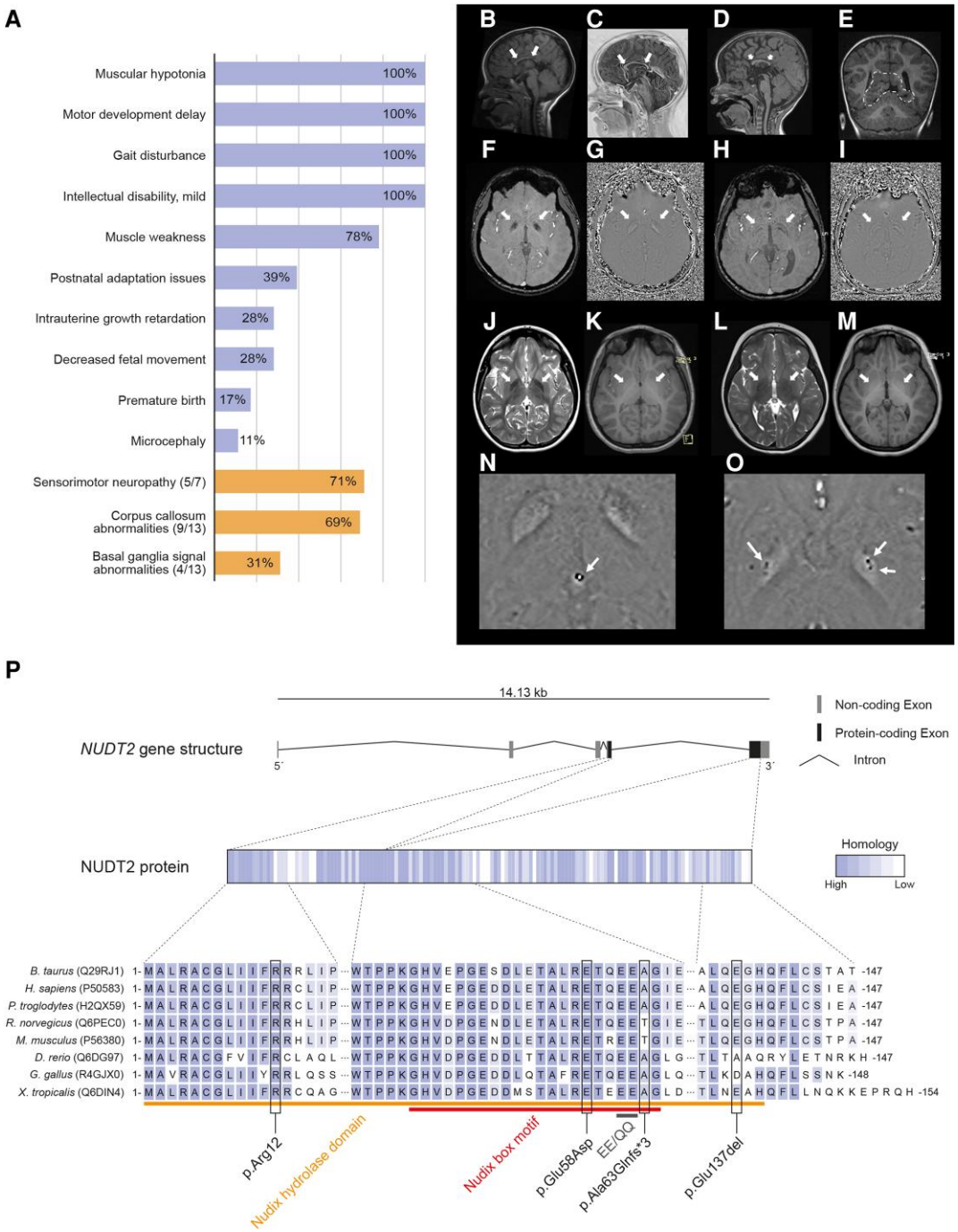

Figure 1 Clinical findings, brain imaging and *NUDT2* structure. (**A**) While dysmorphic features were reported in 13 of 18 individuals, an evaluation of clinical photography by two experienced physicians (F.A., R.A.H.) revealed no recognizable syndrome based on facial gestalt. $n = 18$, unless otherwise noted. (**B–D**) Sagittal T_1 brain imaging of individuals Patients F1:II.3, F3:II.2 and F4:II.2. Hypoplasia (arrows) and/or shorter anterior-posterior length (short arrows) of the corpus callosum was a common abnormality. (**E**) Coronal T_1 imaging. Occipital midline malformation with dysgyria (dashed line) in Patient F1:II.5. (**F–M**) Globus pallidus bilateral-symmetric signal abnormalities (arrows) in axial scans with low signal in susceptibility-weighted imaging (SWI) (**F**, Patient F3:II.1; **H**, Patient F3.II.2), moderately high signal in phase-contrast (**G**, Patient F3:II.1; **I**, Patient F3.II.2), routine spin echo sequences with low signal in T_2-weighted (**J**, Patient F2:II.1; **L**, Patient F2:II.2) and moderately high signal in T_1-weighted images (**K**, Patient F2:II.1; **M**, Patient F2:II.2). Additionally, Patient F3:II.1 showed bilateral-symmetric susceptibility artefacts in the substantia nigra (not shown). Interestingly, earlier imaging in Patient F2:II.1 at age 5 years, in Patient F3:II.1 at age 2 years 7 months and in Patient F3:II.2 at age 2 years 9 months did not show these signal abnormalities indicating an occurrence after early childhood. (**N** and **O**) SWI showed disturbance of susceptibility in phase image in Patient F3: II.1 (**N**, detail from **G**, axial slice including pineal gland). *Arrow*: Bright point with dark rim corresponding to calcification in the pineal gland. This finding is caused by the diamagnetic character of calcium. (**O**) *Arrows*: Dark points with bright rim corresponding to small iron deposition. This dipole finding is caused by the paramagnetic character, which is a strong hint of iron deposition. (**P**) *Top*: Gene structure. Protein-coding exons 4 and 5 are highlighted in black. *Middle*: NUDT2 protein sequence with homology grading from conserved (dark blue) to non-conserved (white) amino acids across eight species. *Bottom*: Magnification of selected regions of NUDT2. Nudix hydrolase domain [orange line, 1-139 amino acids (aa)], Nudix box motif (red line, 43–64 aa) of the gene product, position of the engineered null variant (grey line, 61–62 aa), position of identified variants in patients, and conservation of affected amino acids across different species (black boxes).

Specific findings in susceptibility-weighted imaging (SWI) were indicative of abnormal accumulation of iron or other paramagnetic inorganic substances[22] in the globus pallidus (Fig. 1N and O). Laboratory investigations, including iron and copper metabolism, showed no abnormalities.

Genetic analysis

Standard genomic diagnostic work-up of 13 unreported individuals failed to detect likely pathogenic variants in established disease genes. Prioritizing biallelic non-synonymous variants with a minor allele frequency <0.1% without homozygous occurrence in gnomAD as well as in-house exome and genome datasets from individuals with unrelated phenotypes, we detected rare homozygous variants in *NUDT2* (NM_001161.5) in all affected individuals (Table 1 and Supplementary Table 2) including novel missense c.174G > T (p.Glu58Asp) and in-frame deletion c.410_412del (p.Glu137del) variants. Segregation analyses showed autosomal-recessive inheritance (Supplementary Fig. 1). In line with the homozygous genotype, consanguinity has been reported in 5 of 9 families (Families F1, F2, F8, F9 and F10). The changes p.Ala63Glnfs*3 (Families F4–F9 of European and northern African origin) and p.Arg12* (Families F1 and F2 of Arab-Saudi origin) were identified in several families. While the change p.Arg12* is most likely a founder variant, as indicated by previously reported haplotype analysis,[15] identification of p.Ala63Glnfs*3 in families of different ethnicities without extended runs of homozygosity and overlapping haplotypes renders this variant a likely recurrent change.

Functional characterization of *NUDT2* variants

To address a putative causal link between *NUDT2* alterations and disease, we investigated the functional properties of NUDT2 variant proteins. Variants p.Arg12* and p.Ala63Glnfs*3 result in premature stop codons and likely no functional protein product (Supplementary Fig. 2A). p.Glu58Asp is located within the Nudix box motif (Fig. 1P), affecting a critical residue required for catalysis (Supplementary Fig. 2B).[23] While these variants are predicted to cause loss-of-function, the consequences of the in-frame deletion p.Glu137del, resulting in the loss of Glu137, are less clear. Structural considerations predict a conformation stabilizing role of Glu137 as it interacts with Arg78 on the adjacent β5 strand (Supplementary Fig. 2B). In line with these predictions, NUDT2 protein was absent from patient fibroblasts harbouring variants p.Arg12* and p.Ala63Glnfs*3 (Fig. 2A), while NUDT2 was detected in fibroblasts from patients carrying variant p.Glu58Asp. Plasmid transfections confirmed expression of the p.Glu58Asp and p.Glu137del variants, albeit at much decreased levels for the latter (Supplementary Fig. 2C). These findings showed that variants p.Arg12* and p.Ala63Glnfs*3 do not yield NUDT2 protein while variants p.Glu58Asp and p.Glu137del give rise to full-length protein.

Mutant NUDT2 proteins show severely diminished enzymatic activity

To determine whether NUDT2 mutants were enzymatically active, $NUDT2^{p.Glu58Asp}$ and $NUDT2^{p.Glu137del}$ variant proteins were purified from *Escherichia coli* (Fig. 2B) and tested in *in vitro* activity assays together with wild-type NUDT2 and the catalytically inactive mutant $NUDT2^{EE/QQ}$ as positive and negative controls, respectively.[7] Both variants were essentially devoid of enzymatic m^7G-RNA decapping activity, confirming loss-of-function (Fig. 2C). In addition to decapping, NUDT2 exhibits hydrolase activity towards Ap4A, a side product of aminoacyl-tRNA loading reactions.[24] As shown in Fig. 2D, $NUDT2^{p.Glu58Asp}$ and $NUDT2^{p.Glu137del}$ possessed little to no detectable Ap4A hydrolase activity. We conclude that *NUDT2* variants associated with a neurodevelopmental disorder have an underlying loss-of-function due to lack of protein expression or loss of enzymatic activity.

We investigated the subcellular distribution of NUDT2 and whether this was altered in the pathogenic variants. Increasing evidence indicates that mRNA processing machineries localize to discrete structures, including processing bodies (P-bodies) that can be formed by phase separation in the cytosol.[25] Consistently, heterologously expressed NUDT2 accumulated at punctate cytosolic structures (Supplementary Fig. 3). While $NUDT2^{p.Glu58Asp}$ largely co-localized with wild-type NUDT2, $NUDT2^{p.Glu137del}$ distributed to larger, horseshoe-shaped structures that were clearly different from the foci decorated by wild-type NUDT2. Thus, in addition to the reduction in enzymatic decapping activity, $NUDT2^{p.Glu137del}$ featured an aberrant subcellular distribution.

Altered transcriptome in patient-derived fibroblasts harbouring *NUDT2* variants

Loss of NUDT2 decapping activity suggests that *NUDT2* variant cells could possess an altered transcriptome of mRNAs. To test this possibility, mRNA was isolated from immortalized patient fibroblasts (F1:II.3/p.Arg12* and F3:II.1/p.Glu58Asp) and control wild-type immortalized fibroblasts and subjected to next generation sequencing. Volcano plots (Fig. 2E) show reference transcripts with at least a 2-fold change in expression level and ≤5% FDR in NUDT2 mutant compared to control cells. Distribution of overlapping transcripts elevated in both cell lines identified 37% congruency between the two NUDT2 variants (Fig. 2F and Supplementary Table 3). Gene ontology (GO) pathway analysis using high stringency (FDR ≤5%, ≥10 transcripts per term) identified five major biological process (BP) terms with the most prevalent within embryonic morphogenesis, interferon (IFN) and antiviral responses (Fig. 2G). To validate the RNA-seq data, three upregulated transcripts and one unaltered transcript were randomly selected (Fig. 3A) and their mRNA levels assessed by qRT-PCR in the different cell lines. Consistent with RNA-seq data, mRNA levels were significantly elevated in p.Glu58Asp and p.Arg12* cells, except for the LIMK2 mRNA, which was unaltered in RNA-seq analysis (Fig. 3A). In addition, stability of all three mRNAs, but not of the unaltered LIMK2 mRNA, was increased in cells with disrupted NUDT2 catalytic activity, pointing to a reduced degradation rate (Fig. 3B). Validation analysis of eight additional transcripts found to be elevated in NUDT2 mutant cells by RNA-seq analysis further confirmed the validity of the analysis (Supplementary Fig. 4). To delineate whether the observed reduction in mRNA stability was a consequence of reduced mRNA decapping or defective Ap4A hydrolysis and consequently aberrant accumulation of Ap4A, we utilized the *Arabidopsis thaliana* NUDX26 (AtN26) protein. AtN26 possesses robust Ap4A hydrolase activity (Ogawa *et al.*[26] and Fig. 3C) but minimal to no mRNA decapping activity (Fig. 3D). Stably transformed p.Glu58Asp cell lines that expressed either EGFP, AtN26 or catalytically dead AtN26 ($AtN26^{EE/QQ}$) were generated and used. As shown in Fig. 3E, Ap4A levels were elevated in the Nudt2 defective E58D cells relative to control cells. Importantly, expression of AtN26 but not the catalytically inactive $AtN26^{EE/QQ}$ reduced Ap4A levels to that observed in control cells demonstrating AtN26 can complement the loss of NUDT2 and reduce cellular Ap4A levels. Significantly, analysis of mRNAs used

Table 1 Detailed information on *NUDT2* variants detected in the patient cohort

NUDT2	Variant 1	Variant 2	Variant 3	Variant 4
DNA change (NM_001161.5)	c.34C > T	c.174G > T	c.186del	c.410_412del
Protein change (NP_001152.1)	p.Arg12*	p.Glu58Asp	p.Ala63Glnfs*3	p.Glu137del
IUPAC one letter code	R12*	E58D	A63Qfs*3	E137del
Genomic location (GRCh38)	9-34339073-C-T	9-34343170-G-T	9-34343182-GA-G	9-34343406-34343408-CAAG-C
Reference/variant codon sequence[a]	C**G**A/T**G**A	G**A**G/G**A**T	G**AA**/G**A**	G**AAG**GA/GGA
Variant type	nonsense/stop-gain	missense	frameshift	in-frame deletion
Allele frequency (gnomAD version)	0.000006571 (v3.1.2)	0.00001972 (v3.1.2)	0.0001153 (v2.1.1)	0.000008085 (v2.1.1)
In silico prediction CADD PHRED	36.0	24.4	26.6	-
Conservation score phyloP	3.03	2.88	9.08	5.27
ACMG, IARC classification	Class 5, p	Class 4, lp	Class 5, p	Class 4, lp
ClinVar Variation ID no. of submissions	1686822, 1[b]	2446368, 1[c]	689658, 3 p, 3 lp[d]	2506450, 1[e]
Affected families	F1, F2	F3	F4, F5, F6, F7, F8, F9	F10

CADD PHRED deleterious threshold >10–20. phyloP: positive scores = conserved nucleotide; negative scores = fast-evolving site. p = pathogenic; lp = likely pathogenic.
[a]Positions affected in the respective variant are highlighted in bold.
[b]Family F2 from our cohort and Yavuz *et al.*[15]
[c]Family F3 from our cohort.
[d]Including Family F8 from our cohort.
[e]Family F10 from our cohort.

in Fig. 3A revealed comparable steady state levels regardless of whether the cells expressed wild-type or catalytically inactive AtN26 (Fig. 3F) and consistent with the premise that altered mRNA levels are not a consequence of Ap4A accumulation in the NUDT2 loss-of-function cells. These results support the concept that NUDT2 is a true decapping protein that directly, and possibly indirectly, modulates the stability of a specific subset of target mRNAs.

Discussion

Our study focuses on 18 patients from 10 unrelated families, presenting a consistent neurological clinical pattern with onset of symptoms within the first 1.5 years of life, harbouring four independent, rare, evolutionary conserved, homozygous *NUDT2* variants. Clinical features in all patients were muscular hypotonia, motor developmental delay, gait disturbance and mild intellectual disability. Muscle weakness, sensorimotor neuropathy and corpus callosum abnormalities were present in 78%, 71% and 69% of the patients, respectively. These observed clinical findings are in line with those from previous reports of patients with homozygous *NUDT2* variants.[14-16] Notably, there were indications of basal ganglia iron deposition in one-third of the patients investigated. Gait disturbance and distal muscular atrophy in the legs due to peripheral neuropathy are likely to be progressive, as are basal ganglia changes. We postulate a common mechanism leading to damage of both the central and peripheral nervous systems.

So far, a NUDT2-associated disorder has only been described clinically and genetically. Our biochemical and cell biological findings strongly support that loss of NUDT2 function is common to all identified variants and a likely cause of disease. Loss-of-function resulted from premature translation termination preventing expression of NUDT2 protein or from a severe reduction in enzymatic activity. The undistinguishable pathophysiological consequences of both scenarios suggests that the aetiology of the neurodevelopmental symptoms is due to loss of NUDT2 enzymatic activity. Given the role of NUDT2 in mRNA decapping, it is reasonable to expect that NUDT2-decapped mRNAs will have greater stability and a longer lifespan in patient cells. Consistent with this premise, 602 transcripts were found to be elevated in NUDT2 mutant cells (Supplementary Table 3) and a subset of mRNAs tested from this population exhibited enhanced mRNA stability in the absence of NUDT2 function. Alternatively, loss of NUDT2 activity could also manifest in increased Ap4A levels and signalling. Our Ap4A measurements confirm this premise and show that NUDT2 may be a key player in the regulation of cellular Ap4A levels. The precise function(s) of Ap4A as second messenger is poorly understood. Previous findings linked Ap4A accumulation to stress responses and the regulation of gene expression, DNA repair and immune responses.[27] Our experiments using a novel hydrolase that discriminates decapping activity and Ap4A hydrolysis strongly indicate that the observed increased mRNA stability and concomitant transcript changes are primarily a consequence of defective NUDT2-dependent mRNA decapping. Although compensatory effects by other decapping enzymes cannot be ruled out, these results support that NUDT2 acts in mRNA decapping and indicate that its decapping activity may contribute to the neurodevelopmental disorder presented here.

Accumulating evidence suggests that NUDT2 may be involved in various aspects of the host immune response. NUDT2 reportedly trims off phosphates from 5'-triphosphate-capped viral RNAs, promoting their degradation.[28] Others reported a role of NUDT2 in

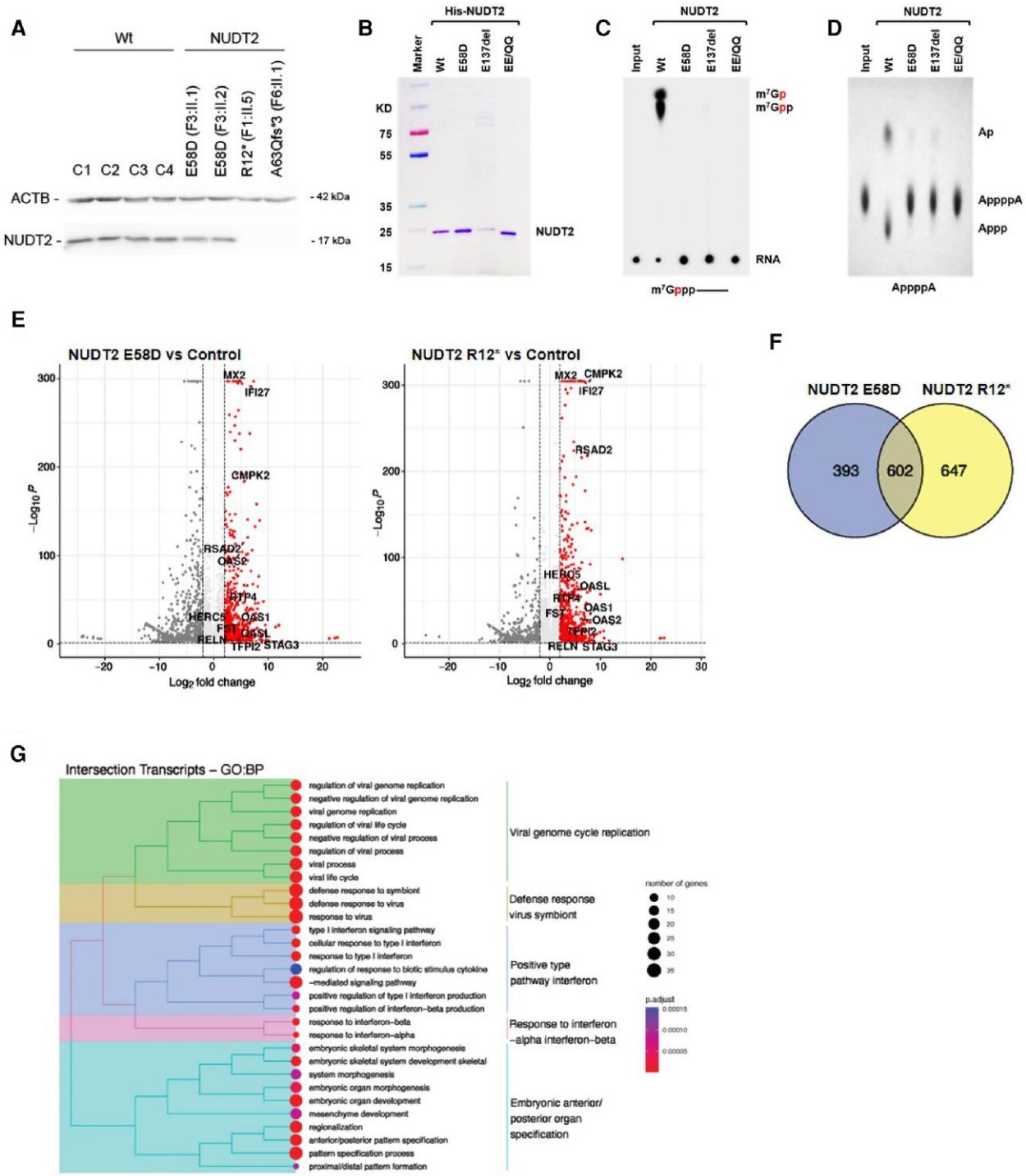

Figure 2 Characterization of NUDT2 variant proteins. (**A**) Immortalized fibroblasts from four healthy controls (Controls C1-C4) and Patients F3:II.1 (p.Glu58Asp), F3:II.2 (p.Glu58Asp), F1:II.5 (p.Arg12*) and F6:II.1 (p.Ala63Glnfs*3) were lysed and processed for western blot detection of NUDT2 and ACTB as loading control. (**B**) Coomassie blue stain of indicated NUDT2 mutant proteins purified from *E. coli*. (**C**) Decapping assay using radiolabelled m^7Gppp-RNA as a substrate (^{32}P denoted in red) and 50 nM of the indicated recombinant protein. Samples were resolved by thin layer chromatography (TLC). Migration of the NUDT2 decapping reaction products, m^7Gp and m^7Gpp are marked. (**D**) Hydrolase assay using 100 nM of the indicated recombinant proteins in the presence of 5 mM Ap4A. Reaction products were resolved by TLC and visualized under short UV light. The position of Ap4A and the two reaction products Ap and Appp is marked. (**E**) Volcano plot of transcripts altered as a consequence of the NUDT2 variants relative to wild-type (Wt) control cells. The log2 fold change is plotted versus the −log10 FDR (false discovery rate). Each transcript is indicated as a dot on the plot. Dots above the horizontal dashed line are <5% FDR. The vertical dashed lines indicate ±4-fold differences. Dots to the right of the +4-fold line are coloured red and to the left of the −4-fold are coloured in grey (only if they are detected with at least 10 mean counts). Transcripts validated in Fig. 3 and Supplementary Fig. 4 are labelled with gene symbols. (**F**) Venn diagram of elevated transcripts from **E** (dots coloured red) from each variant. (**G**) Tree plot of Gene Ontology Biological Process (GO-BP) enriched terms generated from transcripts upregulated in common in **E**. Size of the circles represent the number of genes in each category and the colour of the circles reflect *P*-value of enrichment, as calculated using the clusterProfiler package in R and plotted using the enrichplot package.

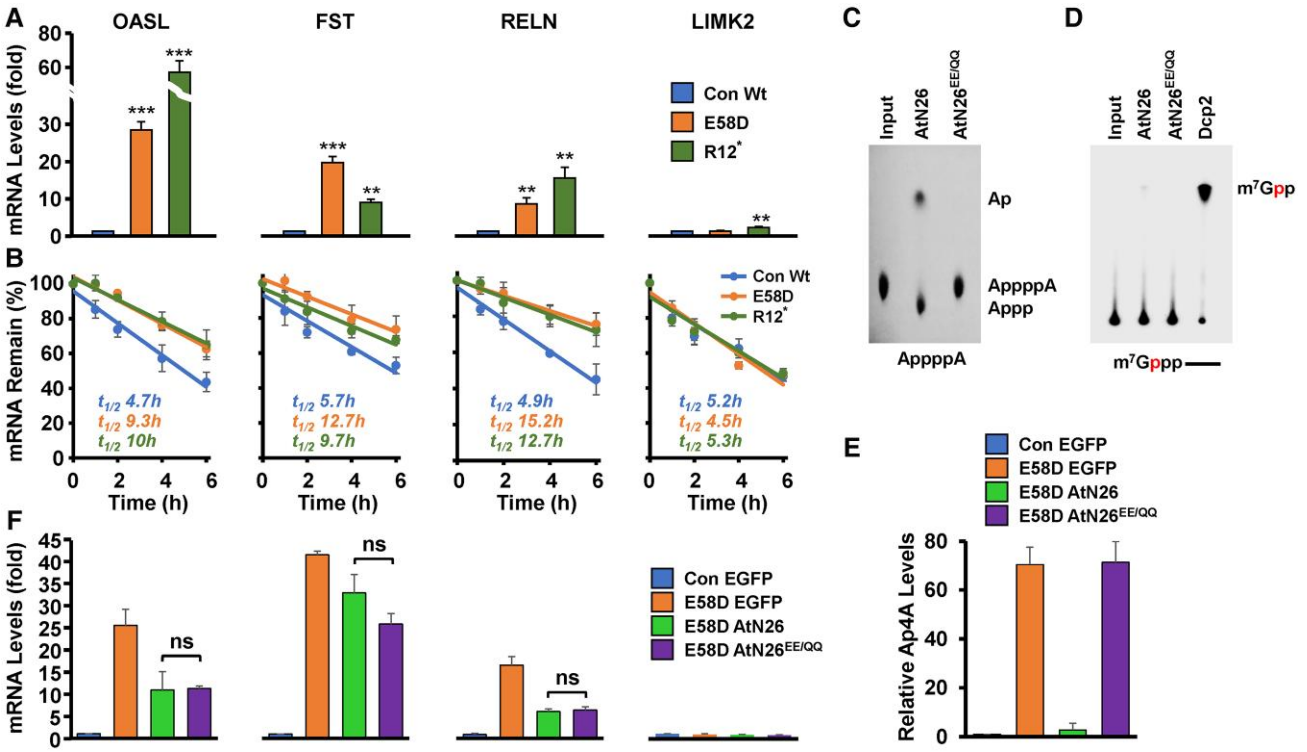

Figure 3 A subset of mRNAs affected by NUDT2 decapping but not by changes in Ap4A levels in NUDT2 variant cells. (**A**) Selected mRNA steady state levels were determined by qRT-PCR and normalized to endogenous GAPDH. mRNA levels in control fibroblast (Con Wt) were set to 1. (**B**) Disruption of NUDT2 decapping alters mRNA stability. mRNA levels were analysed by qRT-PCR at 0, 2, 4 and 6 h following gene transcription inhibition with Actinomycin D. The activity of recombinant wild-type AtN26 or the catalytically inactive AtN26$^{EE/QQ}$ mutant on Ap4A (**C**) or capped mRNA (**D**) is shown where Ap4A hydrolysis and not mRNA decapping is evident. Experimental conditions were as described in the legend to Fig. 2C and D. Dcp2 decapping enzyme was included as positive control in the decapping reactions. (**E**) Fold distribution of Ap4A levels in the indicated cell lines is shown relative to the levels in control cells set to 1. (**F**) Steady state levels of the same four selected mRNAs as in **A**, in the indicated cell lines. mRNA analysis was performed as described for **A**. Error bars show the standard deviation of three independent experiments ($n = 3$ replicates). $^{**}P \leq 0.01$; $^{***}P \leq 0.001$. ns = not significant.

dendritic cell function mediated by its Ap4A hydrolase activity.[29] Our findings that the majority of NUDT2-responsive mRNAs uncovered in p.Glu58Asp and p.Arg12* cells were related to immunity, ranging from interferon response, viral defence mechanisms to regulation of viral replication (Fig. 2G), support the possibility that dysregulated immunity contributes to disease aetiology. In particular, the observed upregulation of IFN-related genes in NUDT2 mutant cells may point to dysfunctional IFN signalling as a factor contributing to disease development. It is noteworthy that a link between defective mRNA degradation and neurodevelopmental disorders in humans is not unprecedented, as illustrated by syndromes associated with *SMG8* and *SMG9*, two components of the nonsense-mediated decay pathway of mRNA degradation.[30] Together with the findings reported here, a picture emerges in which inadequate control of mRNA degradation and homeostasis may be a central theme in the aetiology of congenital neurological disorders.

Data availability

DNA sequence datasets have been generated and contributed by different study sites and have not generally been deposited in a public repository due to varying local consent regulations. For Family F5, genome sequencing data are available in the National Genomic Research Library (https://doi.org/10.6084/m9.figshare.4530893.v6). Selected datasets will be made available by the corresponding author on reasonable request. Novel variants were submitted to the ClinVar database (https://www.ncbi.nlm.nih.gov/clinvar; accession numbers: VCV002446368.2; VCV002506450.1). RNA sequencing data are deposited in GEO (Gene Expression Omnibus, https://www.ncbi.nlm.nih.gov/geo/, accession number: GSE230789).

Acknowledgements

We thank all patients and families for their participation. We thank Andrea Dieckmann, Oliver Hanemann, and Mais Omar Hashem for providing clinical information, Oliver Ohlenschläger for technical assistance regarding the 3D structure, Brenda Huppke for revising the manuscript, and Margit Leitner for technical editing.

Funding

T.B.H.: Deutsche Forschungsgemeinschaft (DFG, German Research Foundation) – 418081722, 433158657. J.G.: doctoral scholarship from the Interdisciplinary Center of Clinical Research (IZKF), Jena University Hospital. M.K.: National Institutes of Health grant GM149262. R.W.T.: Wellcome Centre for Mitochondrial Research (203105/Z/16/Z), UK NHS Highly Specialised Service for Rare Mitochondrial Disorders of Adults and Children. C.A.H.: DFG (HU 800/15-1). A.W.E.: Seed Research Project No. 2101090288, Research and Graduate Studies, University of Sharjah. S.E., R.M. and H.H.:

The Wellcome Trust, The MRC, The MSA Trust, The Michael J. Fox Foundation.

Competing interests

C.B. and P.B. are employees of Centogene AG, Rostock, Germany, a private company which generates revenue from clinical genetic testing. The remaining authors report no competing interests related to the content of this manuscript.

Supplementary material

Supplementary material is available at *Brain* online.

References

1. Kapur M, Ackerman SL. mRNA translation gone awry: Translation fidelity and neurological disease. *Trends Genet*. 2018;34:218-231.
2. Kumar S, Mohapatra T. Deciphering epitranscriptome: Modification of mRNA bases provides a new perspective for post-transcriptional regulation of gene expression. *Front Cell Dev Biol*. 2021;9:628415.
3. Weil D, Piton A, Lessel D, Standart N. Mutations in genes encoding regulators of mRNA decapping and translation initiation: Links to intellectual disability. *Biochem Soc Trans*. 2020;48:1199-1211.
4. Shuman S. Structure, mechanism, and evolution of the mRNA capping apparatus. *Prog Nucleic Acid Res Mol Biol*. 2001;66:1-40.
5. Shatkin AJ, Manley JL. The ends of the affair: Capping and polyadenylation. *Nat Struct Biol*. 2000;7:838-842.
6. Ramanathan A, Robb GB, Chan SH. mRNA capping: Biological functions and applications. *Nucleic Acids Res*. 2016;44:7511-7526.
7. Song MG, Bail S, Kiledjian M. Multiple Nudix family proteins possess mRNA decapping activity. *RNA*. 2013;19:390-399.
8. Grudzien-Nogalska E, Kiledjian M. New insights into decapping enzymes and selective mRNA decay. *Wiley Interdiscip Rev RNA*. 2017;8:10.1002/wrna.1379.
9. Stevens A. Purification and characterization of a Saccharomyces cerevisiae exoribonuclease which yields 5'-mononucleotides by a 5' leads to 3' mode of hydrolysis. *J Biol Chem*. 1980;255:3080-3085.
10. Li Y, Kiledjian M. Regulation of mRNA decapping. *Wiley Interdiscip Rev RNA*. 2010;1:253-265.
11. Ahmed I, Buchert R, Zhou M, et al. Mutations in DCPS and EDC3 in autosomal recessive intellectual disability indicate a crucial role for mRNA decapping in neurodevelopment. *Hum Mol Genet*. 2015;24:3172-3180.
12. Ng CK, Shboul M, Taverniti V, et al. Loss of the scavenger mRNA decapping enzyme DCPS causes syndromic intellectual disability with neuromuscular defects. *Hum Mol Genet*. 2015;24:3163-3171.
13. Salamon I, Palsule G, Luo X, et al. mRNA-Decapping associated DcpS enzyme controls critical steps of neuronal development. *Cereb Cortex*. 2022;32:1494-1507.
14. Anazi S, Maddirevula S, Faqeih E, et al. Clinical genomics expands the morbid genome of intellectual disability and offers a high diagnostic yield. *Mol Psychiatry*. 2017;22:615-624.
15. Yavuz H, Bertoli-Avella AM, Alfadhel M, et al. A founder nonsense variant in NUDT2 causes a recessive neurodevelopmental disorder in Saudi Arab children. *Clin Genet*. 2018;94(3–4):393-395.
16. Diaz F, Khosa S, Niyazov D, et al. Novel NUDT2 variant causes intellectual disability and polyneuropathy. *Ann Clin Transl Neurol*. 2020;7:2320-2325.
17. Sharma S, Grudzien-Nogalska E, Hamilton K, et al. Mammalian Nudix proteins cleave nucleotide metabolite caps on RNAs. *Nucleic Acids Res*. 2020;48:6788-6798.
18. Sobreira N, Schiettecatte F, Valle D, Hamosh A. GeneMatcher: A matching tool for connecting investigators with an interest in the same gene. *Hum Mutat*. 2015;36:928-930.
19. Landrum MJ, Chitipiralla S, Brown GR, et al. ClinVar: Improvements to accessing data. *Nucleic Acids Res*. 2020;48(D1):D835-D844.
20. Wang Z, Kiledjian M. Functional link between the mammalian exosome and mRNA decapping. *Cell*. 2001;107:751-762.
21. Shuman S. Catalytic activity of vaccinia mRNA capping enzyme subunits coexpressed in Escherichia coli. *J Biol Chem*. 1990;265:11960-11966.
22. Deistung A, Mentzel HJ, Rauscher A, Witoszynskyj S, Kaiser WA, Reichenbach JR. Demonstration of paramagnetic and diamagnetic cerebral lesions by using susceptibility weighted phase imaging (SWI). *Z Med Phys*. 2006;16:261-267.
23. Ge H, Chen X, Yang W, Niu L, Teng M. Crystal structure of wild-type and mutant human Ap4A hydrolase. *Biochem Biophys Res Commun*. 2013;432:16-21.
24. Lee YN, Nechushtan H, Figov N, Razin E. The function of lysyl-tRNA synthetase and Ap4A as signaling regulators of MITF activity in FcepsilonRI-activated mast cells. *Immunity*. 2004;20:145-151.
25. Standart N, Weil D. P-Bodies: Cytosolic droplets for coordinated mRNA storage. *Trends Genet*. 2018;34:612-626.
26. Ogawa T, Yoshimura K, Miyake H, et al. Molecular characterization of organelle-type Nudix hydrolases in Arabidopsis. *Plant Physiol*. 2008;148:1412-1424.
27. Ferguson F, McLennan AG, Urbaniak MD, Jones NJ, Copeland NA. Re-evaluation of diadenosine tetraphosphate (Ap(4)A) from a stress metabolite to bona fide secondary messenger. *Front Mol Biosci*. 2020;7:606807.
28. Laudenbach BT, Krey K, Emslander Q, et al. NUDT2 initiates viral RNA degradation by removal of 5'-phosphates. *Nat Commun*. 2021;12:6918.
29. Shu S, Paruchuru LB, Tay NQ, et al. Ap(4)A regulates directional mobility and antigen presentation in dendritic cells. *iScience*. 2019;16:524-534.
30. Abdel-Salam GMH, Duan R, Abdel-Hamid MS, et al. Expanding the phenotypic and allelic spectrum of SMG8: Clinical observations reveal overlap with SMG9-associated disease trait. *Am J Med Genet A*. 2022;188:648-657.